Concurrent photonic measurement of angle-of-arrival and chirp rate of microwave LFM signal

Shangyuan Li (李尚远)*, Haidong Cao (曹海东), and Xiaoping Zheng (郑小平)

Beijing National Research Center for Information Science and Technology, Department of Electronic Engineering, Tsinghua University, Beijing 100084, China

**Corresponding author: syli@mail.tsinghua.edu.cn*

Received April 23, 2020; accepted September 11, 2020; posted online October 23, 2020

A photonic approach to concurrently measure the angle-of-arrival (AOA) and the chirp rate of a linear frequency modulated (LFM) signal is proposed and experimentally demonstrated. The measurement is achieved by estimating the differential frequency of a two-tone signal output by a dual-parallel Mach–Zehnder modulator and an additional asymmetry Mach–Zehnder interferometer. Experiments show that the AOA and the chirp rate are measured simultaneously, with an AOA measurement error of ±0.1° at an signal-to-noise ratio (SNR) of 9.6 dB. When the SNR is −10.4 dB, the AOA error is ±1.3°, and the chirp rate, measured as 210.2 ± 1.5 Hz/ps, has a standard deviation of 0.7%. The measured chirp rate agrees well with the real LFM signal.

Keywords: microwave photonics; interferometer; angle of arrival; linear frequency modulation.
doi: 10.3788/COL202018.123902.

Measurement of angle-of-arrival (AOA) or equivalently time-difference-of-arrival (TDOA) of a microwave signal is of great importance in radio monitoring, electronic warfare, and radar systems. Conventional methods to measure the AOA in the electronic domain use digital sampling of the analog radio signal received by two or more antennas. The sampled signals are digitally processed with a proper estimation algorithm to find the AOA[1]. When processing signals with higher center frequency and larger bandwidth, these methods are facing difficulties from limited sampling rate, insufficient bandwidth of devices, and massive calculation[2,3].

In recent years, several approaches to measure the AOA of microwave signals using microwave photonics technology are proposed[4–6] based on electro-optic modulators and phase-to-intensity mapping. However, the conversion from phase to AOA depends strictly on the frequency of the microwave signal to be measured, and the phase of a microwave signal is vital and can be easily distorted. Thus, the measurement error of the AOA using phase-to-intensity mapping is relatively high. Subsequently, the center frequency should be known or measured in advance, which is difficult to achieve for wideband signals.

Besides, several methods have been proposed to measure the AOA of broadband signals[7–10]. By scanning the phase of the optical side-band, the measurement errors in Ref. [9] are about $< 2.27°$ for a 10 GHz single-tone signal and $< 4.45°$ for 2 GHz broadband signal at 18 GHz. Reference [10] uses voltage at the output of a dual-drive Mach–Zehnder modulator (DD-MZM) and a photodetector to characterize the AOA. The measuring error is about 2°.

For a cooperative measuring system, such as altitude control or landing guidance of aircraft, further improvement of the measurement precision will benefit the application itself[11]. Traditional methods indicate the TDOA or AOA using phase difference, then convert it to intensity. Such a conversion route limits the AOA measurement from better accuracy, due to the phase having a confined range with finite quantification levels. A new indicator and photonic implementation method should be explored to achieve higher accuracy, as well as to meet the bandwidth and frequency requirements from practical applications.

By reviewing methods that can characterize the TDOA or AOA, the linear frequency modulated (LFM) signal shows great potential to convert time or angle to frequency for relatively fast measurement and potentially high speed[12]. Focusing on the AOA measurement of the LFM signal, we tried to measure the frequency, not the phase, to improve the AOA measurement accuracy compared to the conventional method. Two separated antennas receive the LFM signal, and then convert the measuring of the AOA to the measuring of TDOA of the LFM signal. The key to this measurement is to estimate the beat frequency between the two LFM replicas and the chirp rate of the LFM signal simultaneously.

In this Letter, we propose a photonic approach to achieve this measurement based on a dual-parallel Mach-Zehnder modulator (DP-MZM) and an asymmetry Mach-Zehnder interferometer (AMZI) with known differential delay. The problem of characterizing the AOA and the chirp rate is transformed to measure the frequency value of a two-tone signal. By utilizing the frequency, not the phase, to identify the AOA or TDOA, higher measurement accuracy is obtained. The AOA error of the experiment is about ±0.1° at a signal to noise ratio (SNR) of 9.6 dB. It is increased to ±1.3° at an SNR of −10.4 dB. The chirp rate of the LFM signal is also measured and calculated simultaneously, with a well-agreed value of 210.2 ± 1.5 Hz/ps at an SNR of −10.4 dB.

Figure 1 shows the schematic diagram of the whole setup for AOA measurement. The AOA processing system

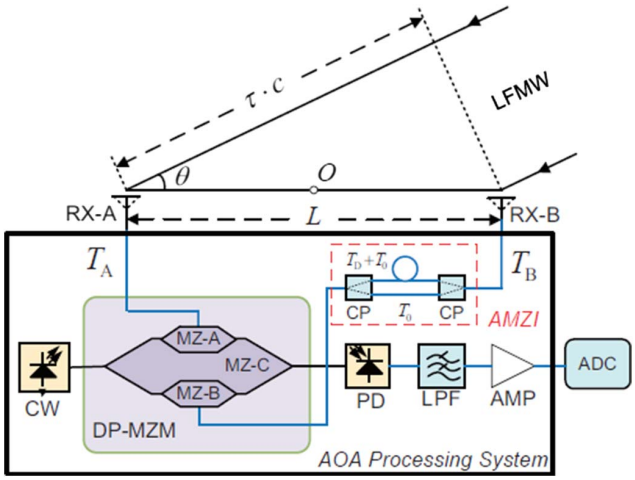

Fig. 1. Scheme diagram of the proposed approach.

(PS) (AOA-PS) is illustrated inside the thick frame, which has two radio frequency (RF) ports (RX-A and RX-B) connected with two RF antennas, located with a distance separation of L. The LFM signal comes from a definite direction with an AOA of θ relative to the baseline through the two antennas. Under the far-field approximation, the incoming LFM signal can be regarded as a plane wave. Therefore, the propagation time difference τ from the signal emitter to both antennas will satisfy

$$\tau = L \cdot \cos\theta / c. \tag{1}$$

This will convert the AOA to TDOA for the AOA-PS.

Further, we could take advantage of the intrinsic feature of an LFM signal to realize the TDOA measurement. An LFM signal can be expressed as

$$s(t) = A\cos\left[2\pi\left(f_0 t + \frac{1}{2}kt^2\right)\right], \tag{2}$$

where f_0 is the initial frequency, k is the chirp rate, and A is the amplitude of the signal. For the LFM signal, the instantaneous frequency changes with time linearly, shown as the blue line in the time-frequency figure in Fig. 2.

When two replicas of an LFM signal with a certain time delay τ multiply each other, a constant frequency f at low frequency can be obtained with proper signal filtering, and satisfy

$$f = k \cdot \tau. \tag{3}$$

This multiplication and filtering procedure is called LFM de-chirp. Accordingly, the measurement of AOA or TDOA is converted to the measurement of the beat frequency, coming from the low-frequency output port and digitized by a low-frequency analog-to-digital converter (ADC), as shown in Fig. 1.

According to Eqs. (2) and (1), we can derive the cosine of the AOA as

$$\cos\theta = f \cdot c / Lk. \tag{4}$$

Therefore, the measuring error of AOA θ can be expressed by

$$\frac{\delta\cos\theta}{\cos\theta} = \frac{\delta f}{f} + \frac{\delta k}{k} + \frac{\delta L}{L}. \tag{5}$$

From Eq. (5), we can see that the relative error of $\cos\theta$ is largely influenced by the relative measuring error of frequency f, chirp rate k, and baseline length L. For a given AOA θ, the longer the baseline is, the smaller the error of θ would be.

The essential function of the AOA-PS is to realize the multiplication and de-chirp of the two LFM signals from both antennas using microwave photonic technology. RX-A and RX-B receive the LFM signal and then drive the two sub-Mach–Zehnder (MZ) structures of the DP-MZM in the AOA-PS.

Supposing the time delay between two signals applied to MZ-A and MZ-B is equal to τ, the modulated RF signals onto MZ-A and MZ-B are $s(t)$ and $s(t+\tau)$, respectively[13]. After photo detection and low-pass filtering, the mixed output can be expressed as

$$i(t) \propto s(t) \cdot s(t+\tau) \xrightarrow{\text{LPF}} \cos 2\pi\left(k\tau t + f_0\tau + \frac{1}{2}k\tau^2\right). \tag{6}$$

In cases where we have fore-knowledge of the chirp rate k of the LFM signal under test, τ can be achieved accordingly.

Nevertheless, for most cases, k is unknown, and especially for moving targets, the received chirp rate k can be different from the transmitted one due to the Doppler phase shift. Hence, τ and θ cannot be calculated. Dealing with this issue, we incorporate an AMZI, which contains two couplers and two transmission lines with a time delay of T_0 and $T_D + T_0$, as shown in Fig. 1. The AMZI makes a time-delayed copy of the input signal and outputs the combined replicas. The differential delay time T_D is measured and determined beforehand.

Note T_A as the transmission time from RX-A to MZ-A. Note T_B as the time from RX-B to MZ-B, except for the AMZI. The transmission time differences between the two replicas in link B and link A satisfy

$$\tau_1 = T_B + T_0 - T_A - \tau, \tag{7}$$

$$\tau_2 = T_B + T_0 + T_D - T_A - \tau, \tag{8}$$

where τ is the AOA induced TDOA, satisfying $\tau = L \cdot \cos\theta / c$.

When one LFM signal multiplies with two time-delayed LFM replicas with τ_1 and τ_2, two beat frequency components of f_1 and f_2 are obtained, as illustrated in Fig. 2. This is a two-tone signal, of which the differential frequency is directly associated with the chirp rate. The frequencies satisfy

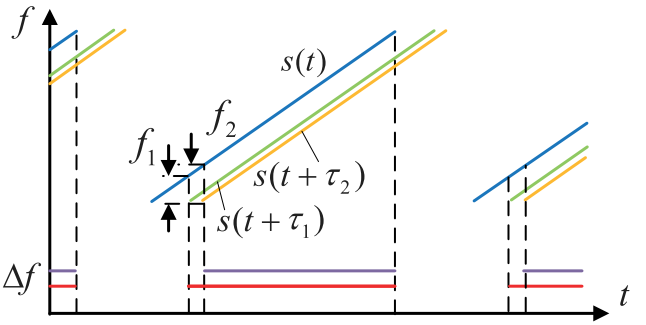

Fig. 2. Frequency-time two-dimensional (2D) image to illustrate the intrinsic feature of an LFM signal, and the dual-frequency generation using AMZI for concurrent measurement of TDOA and chirp rate.

$$f_1 = |k \cdot \tau_1|, \quad f_2 = |k \cdot \tau_2|. \tag{9}$$

If τ_1 and τ_2 are both positive or negative at the same time, $|k|$ can be calculated and expressed as

$$|k| = |f_2 - f_1|/(\tau_2 - \tau_1) = |\Delta f|/T_D. \tag{10}$$

Unfortunately, if τ_1 and τ_2 have opposite signs, miscalculation will occur for both f and k.

To solve this problem, we manage to elongate link B between RX-B and MZ-B to satisfy

$$T_R = T_B + T_0 - T_A > \tau_{\max}, \tag{11}$$

where T_R is the differential time delay of the two links in the AOA-PS; $\tau_{\max} = L/c$ is the maximum AOA induced TDOA of the measurement system. By incorporating such a fixed time delay T_R, this inequation ensures a non-negative τ for any AOA value. This will lead to a frequency bias for the mixing output of the LFM signals. Then, Eq. (9) is transformed to

$$f_1 = |k| \cdot \tau_1, \tag{12}$$

$$f_2 = |k| \cdot \tau_2. \tag{13}$$

The validity of Eq. (10) will be kept consequently.

With all of the setup above, it is possible to calculate $|k|$ and τ simultaneously, since we have two unknown numbers and two measured results, f_1 and f_2. As the AOA θ has a definite relationship with TDOA τ, the final results are

$$\theta = \arccos(\tau \cdot c/L) = \arccos\left[\left(T_R - \frac{T_D \cdot f_1}{|f_2 - f_1|}\right) \cdot c/L\right]. \tag{14}$$

Thus, the chirp rate and the AOA are obtained concurrently.

A proof-of-concept experiment is carried out to verify the proposed approach. The experimental setup is shown in Fig. 3.

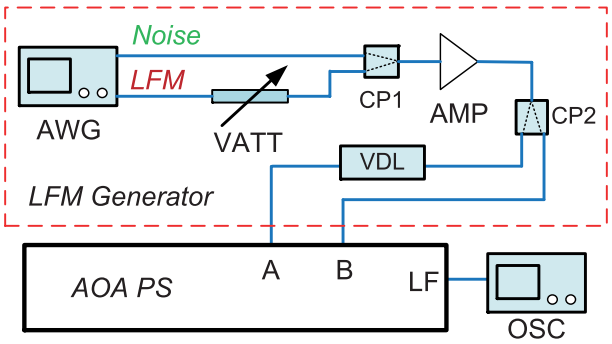

Fig. 3. Diagram of the whole measurement system.

The whole setup consists of three parts, the LFM signal generator, which is placed in the red dashed box, the AOA-PS system, and the ADC frontend, which is an oscilloscope. In the LFM signal generator, the arbitrary waveform generator (AWG, Tektronix AWG72000A) generates both the LFM signal and the noise at a sample rate of 25 Gbps. Channel 1 generates the LFM signal, which occupies a bandwidth of 4 GHz, ranging from 2 GHz to 6 GHz. The pulse repetition rate of the LFM signal is 50 kHz, and the pulse width is 19 μs.

The LFM signal is then attenuated by a variable microwave attenuator (VATT) with an attenuation step of 1 dB and coupled with the noise using an RF coupler. The noise is digitally generated as Gaussian white noise, filtered to occupy the bandwidth from 2 GHz to 6 GHz, and then downloaded to channel 2 of the AWG. The noise power is fixed so that by changing the VATT, the SNR of the coupled signal can be easily controlled. Measured by an RF power meter, the signal power is −5.0 dBm while the VATT is set to 0 dB, and the noise power is −14.6 dBm, resulting in the best SNR of 9.6 dB.

The combined signal and noise are then amplified by a wideband amplifier and divided into two parts using another coupler. The AOA of a signal results in a time delay between the RX antennas. We use several pieces of RF cable to emulate such a variable time delay line (VDL) to generate different AOA states.

In the AOA measurement system, the optical carrier generated by a CW laser is fed into the DP-MZM (Fujitsu FTM7961EX). One copy of the noisy LFM signal from the LFM signal generator drives MZ-A of the DP-MZM. The other copy is fed into the AMZI and then modulates MZ-B of the DP-MZM.

The AMZI utilized in the experiment is composed of two RF couplers and two pieces of coaxial transmission line. The differential delay of the AMZI is measured as $T_D = 4584$ ps.

The waveform of the measured signal is digitized by an oscilloscope (Keysight MSOS804A) at a sampling rate of 200 MSa/s (digitally down-sampled). While the SNR is 9.6 dB (VATT: 0 dB), the low-frequency waveform is shown in Fig. 4(a). The spectrum of the waveform is estimated and shown in Fig. 4(b). Two frequency components

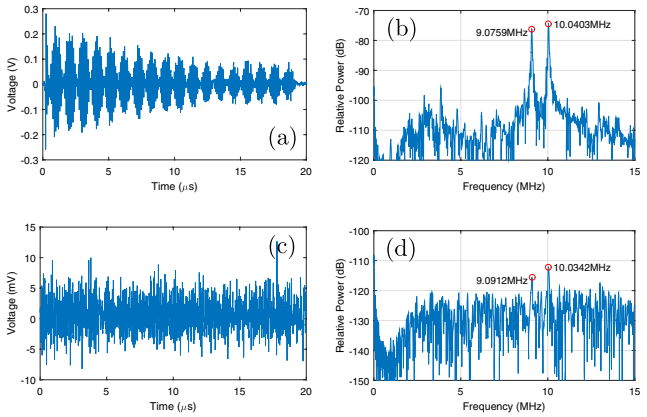

Fig. 4. Waveform and spectrum of the measured signal at different SNRs. (a) Waveform with SNR = 9.6 dB shows the beating of two sinusoidal signals; (b) spectrum with SNR = 9.6 dB shows two frequency peaks; (c) waveform with SNR = −10.4 dB shows nothing but noise in the retrieved signal; (d) spectrum with SNR = −10.4 dB is still able to reveal two frequency components.

are obtained in the spectrum at 9.0759 MHz and 10.0403 MHz, with a differential frequency of 964.4 kHz.

The chirp rate is calculated as 210.4 Hz/ps using Eq. (10). When decreasing the SNR to −10.4 dB (VATT: 20 dB), the measured waveform [Fig. 4(c)] contains almost only noise. However, the two frequency components can still be observed, with a differential frequency of 943.0 kHz, as shown in Fig. 4(d).

We measure and record the waveform 100 times with a time interval of about 1 s at each attenuation from 0 dB to 19 dB. Then, we estimate the spectrum, find the differential frequency between two peak frequency components in each spectrum, calculate the chirp rate according to Eq. (10), and then calculate its statistical characteristics. We illustrate the mean chirp rate and its measurement error in Fig. 5. The best estimation of the chirp rate under the highest SNR is $k = 210.4$ Hz/ps, while the actual value is $k = 4\,\text{GHz}/19\,\mu\text{s} = 210.5$ Hz/ps according to the waveform itself, shown in the dash-dot line in Fig. 5. It is clear that while the SNR decreases, the estimation of k varies a little, but with larger error. When the SNR is −10.4 dB, the chirp rate is 210.2 ± 1.5 Hz/ps, where the standard deviation is about 0.7% of the measurement result.

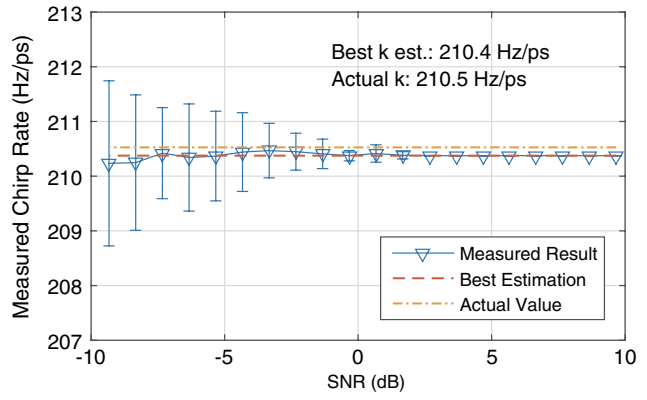

Fig. 5. Measured chirp rate versus SNR.

The chirp rate measurement in the previous subsection only demonstrates the validity of one TDOA status. In the real AOA measurement scenario, TDOA changes along with the AOA. Therefore, it is necessary to verify the feasibility of the method for more TDOA status. By inserting several pieces of transmission line with different time delays in link A, we could emulate different TDOA status, as well as different AOA conditions.

For each time delay, the beat signal should contain two frequency components in the spectrum, as shown in Fig. 6. As the time delay increases, the beat frequency becomes higher, while keeping their frequency difference of 964.4 kHz.

Figure 7 shows the measured AOA results with their errors for different SNRs. At an SNR of 9.6 dB, the measured AOA values agree well with the initiated AOA values, as shown in Fig. 7(a). The maximum AOA error is about ±0.1° for the AOA near 0° and 180° and smaller for the AOA around the perpendicular direction, as shown in Fig. 7(b).

While the SNR equals −10.4 dB, the measured AOA results still correspond well with the initiated value, with a

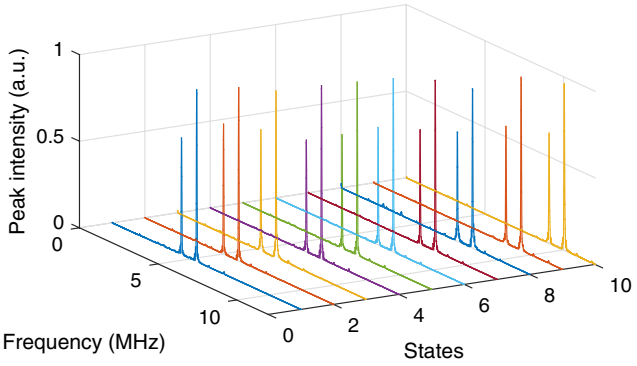

Fig. 6. Measured two-tone spectrum at different time delays.

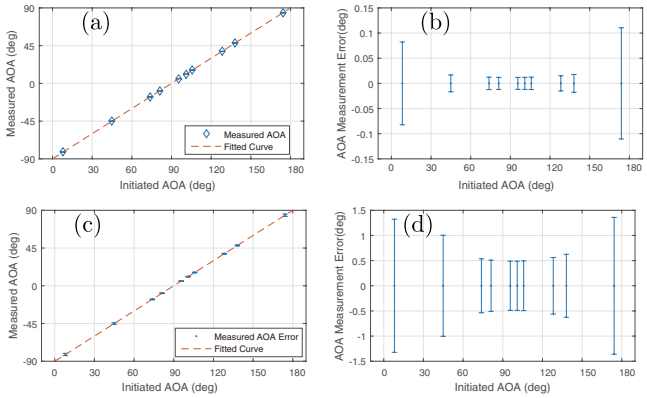

Fig. 7. AOA measurement results and their measurement error at different SNRs. (a) AOA measurement results and (b) measurement error with SNR = 9.6 dB. (c) AOA measurement results and (b) measurement error with SNR = −10.4 dB.

maximum AOA error of ±1.3° for the AOA near 0° and 180°, as shown in Figs. 7(c) and 7(d). It is clear that better SNR will lead to smaller AOA error.

In the experiment, the range of AOA measurement of the proposed scheme is from about 5° to 175°. Because of the cosine relationship between f and θ in Eq. (1), the error of θ increases rapidly when the AOA gets close to 0° or 180°.

In summary, we have proposed a photonic approach to measure the AOA and the chirp rate of an LFM signal received by two separated antennas. Using a DP-MZM to mix the LFM signals and using low-speed ADC to digitize the beat frequencies, this approach can obtain the AOA and the chirp rate simultaneously. In the experiment, the AOA from 5° to 175° with a maximum measurement error of ±0.1° is achieved at an SNR of 9.6 dB, while it is ±1.3° at an SNR of −10.4 dB. The chirp rate is also estimated, having a well-agreed measurement value of 210.2 ± 1.5 Hz/ps. The result indicates a standard deviation of about 0.7% of the measured result. The measured chirp rate agrees well with the real LFM signal. The measurement can be achieved with only one pulse of the LFM waveform, of which the time duration varies from the microsecond level to the millisecond level.

This work was supported by the National Key Research and Development Program of China (No. 2019YFB2203301) and the National Natural Science Foundation of China (No. 61690191/2).

References

1. L. C. Godara, Proc. IEEE **85**, 1195 (1997).
2. M. M. Hyder and K. Mahata, IEEE Trans. Signal Process. **58**, 4646 (2010).
3. Y. Gao, A. Wen, H. Zhang, S. Xiang, H. Zhang, L. Zhao, and L. Shang, Opt. Commun. **321**, 11 (2014).
4. Z. Tu, Z. Xu, A. Wen, X. Li, and S. Zhang, Opt. Eng. **59**, 036110 (2020).
5. P. Li, L. Yan, J. Ye, X. Feng, W. Pan, B. Luo, X. Zou, T. Zhou, and Z. Chen, Opt. Express **27**, 8709 (2019).
6. Y. Ni, X. Kong, R. Wang, Y. Dai, and K. Xu, Chin. Opt. Lett. **11**, 030605 (2013).
7. Z. Tu, A. Wen, Z. Xiu, W. Zhang, and M. Chen, IEEE Photon. J. **9**, 5503208 (2017).
8. H. Chen and E. H. W. Chan, J. Lightwave Technol. **38**, 2292 (2020).
9. P. Li, L. Yan, J. Ye, X. Feng, X. Zou, B. Luo, W. Pan, T. Zhou, and Z. Chen, J. Lightwave Technol. **37**, 6048 (2019).
10. H. Chen and E. H. W. Chan, IEEE Photon. Technol. Lett. **31**, 1795 (2019).
11. T. Zsedrovits, A. Zarandy, B. Vanek, T. Peni, J. Bokor, and T. Roska, J. Intell. Robot. Syst. **69**, 407 (2013).
12. C. Tarran, M. Mitchell, and R. Howard, in *IEE Colloquium on High Resolution Radar and Sonar* (1999).
13. L. Huang, R. Li, D. Chen, P. Xiang, P. Wang, T. Pu, and X. Chen, IEEE Photon. Technol. Lett. **28**, 880 (2016).